Journal of Applied Mechanics Vol. 3, pp. 387-394 (August 2000) JSCE

An Experimental Study on Strain-Based Failure Criteria of Brittle Materials

岩石及びコンクリートにおける歪みに基づく破壊基準の実験的研究

Xiaochun LI*, Zhishen WU**, Manabu TAKAHASHI*** and Kazuya YASUHARA****
李 小春・呉 智深・高橋 学・安原一哉

*Non-Member Doctoral candidate, Dept. Urban & Civil Eng. , Ibaraki Univ.(4-12-1 Nakanarusawa, Hitachi, Ibaraki)
**Member PHD Associate Prof, Dept. Urban & Civil Eng. , Ibaraki Univ.(4-12-1 Nakanarusawa, Hitachi, Ibaraki)
***Member PHD, Dept. Environ. Geol., Geological Survey of Japan (1-1-3 Higashi, Tsukuba, Ibaraki)
**** Member PHD Prof, Dept. Urban & Civil Eng. , Ibaraki Univ.(4-12-1 Nakanarusawa, Hitachi, Ibaraki)

A strain-based criterion can possibly serves as a direct and convenient approach for the stability assessment of geo-structures. The purpose of the present study is to experimentally verify the applicability of 2 strain-based failure criteria : 1) critical tensile strain criterion(Fujii, 1994) and 2) critical strain criterion(Sakurai, 1982) to rocks and concrete. Effects of confining pressure, pore pressure, intermediate principal stress, strain rate on the critical tensile strain ε_{TC} and critical strain ε_0 have been investigated by triaxial tests and true triaxial tests for 2 kinds of Shirahama sandstone and 4 kinds of concretes with different aggregate sizes. The experimental results show that tensile strain ε_{TC} and the critical strain ε_0 are not affected significantly by confining pressure, intermediate principal stress, strain rate and maximum aggregate size under low confining pressure and intermediate principal stress. However, the critical strain ε_0 become higher than the maximum strain at failure ε_{1f} when σ_2 >100MPa, which suggests that critical strain criterion(Sakurai, 1982) may over-estimate load-carrying capacity of structures. In view of this, a new definition of the critical strain has been proposed, which takes the effect of intermediate principal stress into considerations. The proposed definition has a clearer physical meaning and affected by the intermediate principal stress to a less extent than the original one.

Key Words: strain-based failure criterion, rock, concrete

1 Introduction

Failure criteria are of central importance to rock, soil and concrete mechanics, as well as the engineering designs. Considerable efforts have been devoted to the formulation of failure criteria and to their experimental verifications, and various expressions of criteria and models have been proposed. Up to now, in practical mechanical analyses and engineering designs, the stress-based criteria have been predominant, such as Mohr-Coulomb criterion, Hook-Brown criterion[1], and Willian-Warnke criterion[2].

Failure criteria also can be based on strain . Strain-based criteria have significant values in practical engineering. For example, in underground cavity excavations, the information on the strain or deformation of the structures composes the most of monitoring data of structure responses because they are measured more easily than the stresses. The strain-based criteria can serve as a direct and convenient approach for the stability assessment of geo-structures with no need to pre-assume a constitutive equation. Furthermore, the strain-based failure criteria are necessary for the mechanical analysis in strain space.

Although the strain-based criteria were not intensively studied and widely applied in comparison with the stress-based criteria, they have become the subject of some studies in recent years. In the present study, experimental verifications will be made on 2 criteria: tensile strain criterion[3] and critical strain criterion[4], based on our experimental results of several kinds of rocks and concrete under triaxial compressions.

Tensile strain criterion, proposed by Fujii[3], is expressed by the following simple equation.

$$\varepsilon_T = \varepsilon_{TC} \tag{1}$$

where ε_T is the minimum principal strain(tensile) and ε_{TC} is the critical tensile strain defined as the absolute value of ε_T at failure(Fig.1). Note that compressive strain is defined as positive. The equation(1) means that failure occurs when the minimum principal strain reaches the critical value. Although the equa-

tion(1) looks similar to those proposed by St. Venant[5], Carino and Slate[6], Kotte et al[7] and Stacey[8], but tensile strain criterion is different from them in physical meanings[3].

It has been illustrated by Fujii et al.[3),10),11)] and Kiyama et al.[9)] that the values of critical tensile strain ε_{TC} obtained by Brazilian test, uniaxial compressive test, triaxial test and creep test for each of several kinds of rocks show almost same values.

While tensile strain criterion puts its attention to the minimum principal strain, critical strain criterion is associated with maximum principal strain(compressive). In order to assess the stability of tunnels, Sakurai[4)] proposed the so-called direct strain evaluation technique, in which the "critical strain", ε_0 (uniaxial compressive strength divided by modulus of deformation as expressed by equation(3)) plays an important role as an allowable value (Fig.1).

$$\varepsilon_1 = \varepsilon_0 \tag{2}$$

where ε_1 is maximum principal strain and ε_0 is critical strain which can be obtained by uniaxial compressive tests as follows.

$$\varepsilon_0 = \sigma_c / E_i \tag{3}$$

where σ_c is uniaxial compressive strength and E_i is modulus of deformation(Fig.1). The equation(2) means that rock under uniaxial compression tends to fail when the maximum principal strain exceeds the critical value. It has been demonstrated that for same kind of rock , the critical strain of the jointed rock mass measured by in-situ tests is almost equal to that of the intact rock by laboratory tests. This suggests that the critical strain of jointed rock mass can possibly be obtained by laboratory tests[4)].

The critical strain defined as equation(3) shows similar value to that defined as equation(4) in case of triaxial tests for tuff, and it is independent of confining pressure, moisture content, temperature to some extent[12)].

$$\varepsilon_0 = (\sigma_1 - \sigma_3)_f / E \tag{4}$$

where $(\sigma_1-\sigma_3)_f$ is the differential stress at failure, E is modulus of deformation.

The above strain-based criteria are simple in expression and the material constants are ready to be obtained. Whether a criterion is applicable depends on to what extent the material constants are influenced by environmental factors. While the previous work[3),4),9),10),11)] contributed to the experimental investigations of the effects of moisture and time for limited kinds rocks under very low confining pressure, present study has investigated effects of confining pressure, pore pressure, intermediate

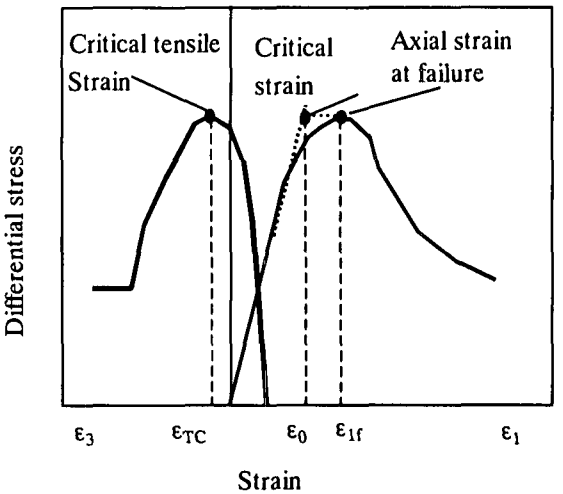

Fig.1 Definitions of critical tensile strain and critical strain

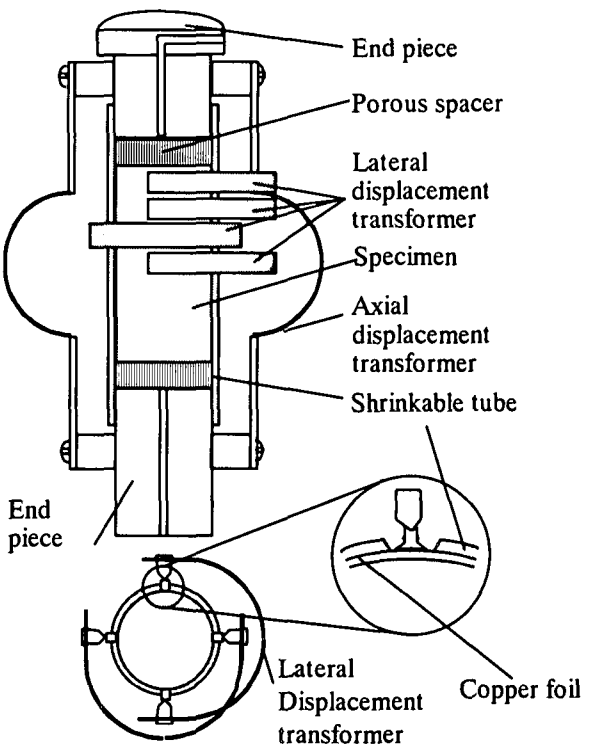

Fig.2 Specimen assembly for conventional triaxial tests

principal stress, strain rate by triaxial tests and true triaxial tests for 2 kinds of Shirahama sandstone and 4 kinds of concretes with different aggregate sizes.

2 Experimental Techniques

Materials investigated are listed in Table 1, including 2 kinds of Shirahama sandstone with porosity about 13% and 4 kinds of concretes with different maximum aggregate sizes. The mix proportions of concrete are given in table 2. The concrete was cast in $\phi 50 \times 100$mm moulds, vibrated, kept in the moulds for 3 days, demoulded and finally immersed in water. At an age of 28

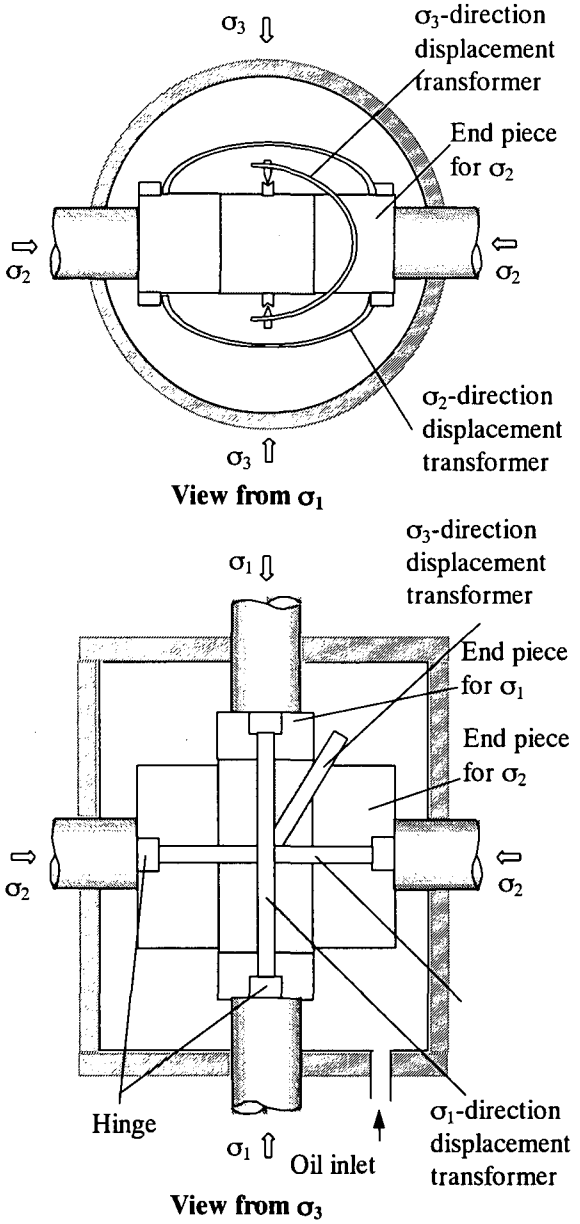

Fig.3 Specimen assembly for true triaxial tests

days, the concrete specimens were taken out of the water, the upper and lower surfaces of the specimens were ground and placed in the laboratory for 3 months to be room dried.

Uniaxial and conventional triaxial tests and true axial tests have been carried out with the apparatuses at Geological Survey of Japan. The apparatus for conventional triaxial tests with an axial loading capacity of 2000KN and a confining pressure capacity of 100MPa, can be used to load a specimen in force control or in deformation control. Specimen assembly for conventional triaxial tests is illustrated as Fig.2. The specimen in the vessel, jacketed with 0.5mm thick shrinkable tube , was connected to a pore pressure system which supplied pore pressure and kept it constant. The deformations of the specimen were measured by 6 cantilever-type displacement transformers, on each of which 4 strain gates in full bridge configuration were mounted. The 2 axial transformers were fixed between 2 end

Table1 Experimental materials and items

Materials	Max. Grain size(mm)	Specimen size(mm)	Test items*
Shirahama sandstone I	0.15	φ30*60	CTT-D, CTT-P
Shirahama sandstone II	0.15	35*35*70	TTT-D
Concrete	1.2	φ50*100	CTT-R
	2.5		CTT-D
	5		
	15		

*: CTT-D, CTT-P: conventional triaxial test for room-dry specimens or with pore pressure respectively. CTT-R: conventional triaxial test under different strain rates. TTT-D: true triaxial test for room-dry specimens .

Table 2 Concrete mix proportions

Max. aggregate size(mm)	W/C (%)	cement (kg/m^3)	Fine aggregates (kg/m^3)	Coarse aggregates (kg/m^3)
15	59.3	184	852	986
5	59.1	295	1355	--
2.5	59.1	295	1355	--
1.2	59.1	295	1355	--

pieces(Fig.2). Therefore, the measured deformation included the deformation of the end pieces and the deformation occurring at specimen-end piece interfaces. The former could be corrected easily. The latter may brought about an overestimation of around 200με. The 4 lateral displacement transformers were installed at different heights and directions of the specimen. To eliminate the effect of the jacket deformation on the measurement of the lateral strain, there were holes in the jacket and 0.05mm thick copper foil was put between the jacket and the specimen to seal the holes. Stainless rods were stuck on the copper foil, on which the lateral transformers were mounted. All the transformers have been calibrated under oil pressure up to 50Mpa. No significant effect of pressure on the sensitivity was found. In conventional triaxial tests, after confining pressure and pore pressure reached prescribed values, the axial stress was loaded in axial deformation control. For Shirahama sandstone I , a constant axial strain rate of 1.4με/s was used, while for concrete, 1, 100, 1000με/s.

The apparatus for true triaxial tests can load 3 principal stresses to a rectangular parallelepiped specimen independently. The maximum and intermediate principal stresses were loaded by 2 pairs of rigid pistons, while the minimum principal stress directly by oil in the vessel(Fig.3). The specimen was jacketed with silicon rubber. A 0.05mm thick Teflon sheet and copper foil were place between the specimen and end pieces to eliminate the frictions. The technique for deformation measurement was similar to that used in conventional triaxial tests. In true

triaxial tests, the load path was as follows. First, 3 principal stresses were loaded simultaneously to a prescribed value by the oil pressure. Then, keeping the oil pressure, i.e. minimum principal stress, constant, the maximum and intermediate principal stresses were synchronously exerted to a prescribed value with them equal to each other, Finally, keeping the minimum and intermediate principal stresses constant, the maximum principal stress was increased at an vertical strain rate of 5με/s until the specimen failed.

3 Experimental Results

3.1 Conventional triaxial tests for Shiraham sandstone I : the effects of confining pressure and pore pressure

Shirahama sandstone I specimens has been deformed under triaxial compression up to a confining pressure of 100Mpa, with or without pore pressure. Fig4 and Fig.5 show differential stress-strain curves for room dry specimens and with pore pressures. Note that in Fig.4(a) and Fig.5(a), the diametrical strain is total strain including the strain occurring due to loading of the confining pressure and pore pressure, while in Fig.4(b) and Fig.5(b), the axial strain is differential strain. It has been observed that the specimen under triaxial compression exhibits non-axisymmetric diametrical deformation with the differential stress increasing and anelastic deformation occurring, in spite of the stress state is axisymmetric. Therefore, the diametrical strain in Fig.4(a) and Fig.5(a) is the higher one of the values measured by 2 lateral displacement transformers perpendicularly installed in the middle height of the specimen(Fig.2) . The figures in Fig.4 are the values of confining pressures, and in Fig.5 are those of confining pressures and pore pressures. With the confining pressure increasing, the differential stress-strain curves show a transition from strain softening to strain-hardening. Meanwhile, it could be observed that a transition in the failure pattern from brittle fracture to uniform ductile deformation. The brittle-ductile transition occurred at an effective confining pressure of about 30MPa. Here, the effective confining pressure means confining pressure minus pore pressure. The tensile strain ε_{TC} and the critical strain ε_0 under different confining pressures and pore pressures are plotted in Fig.6 as a function of the effective confining pressure. The values of the tensile strain ε_{TC} are ε_3 corresponding to the peak point of the stress-strain curves. The values of the critical strain ε_0 were obtained by equation(4), where the modulus of deformation is the slope of the initial linear segment of the stress-strain curves.

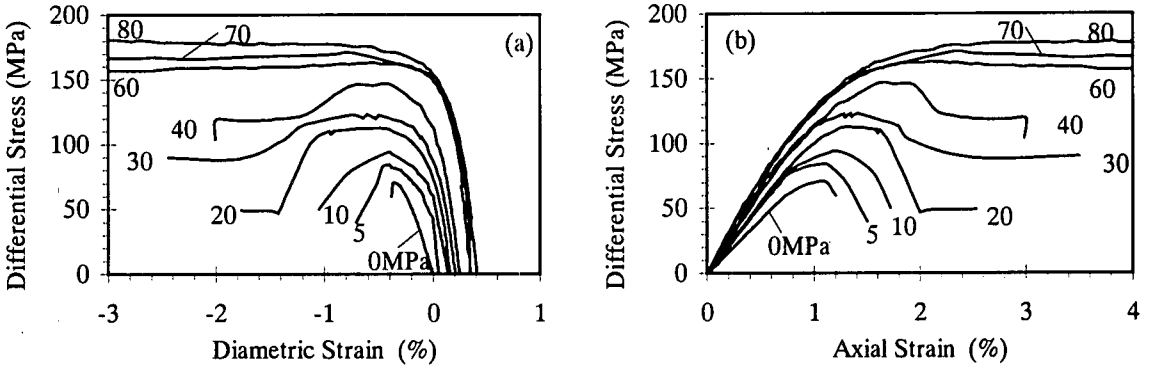

Fig.4 Differential stress-strain curves(Shirahama sandstone I, room dry)

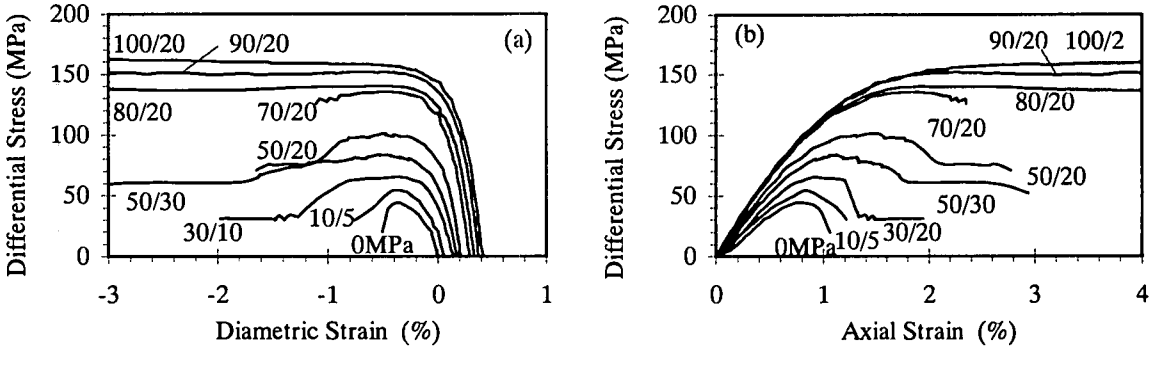

Fig.5 Differential stress-strain curves(Shirahama sandstone I, with pore pressure)

It can be seen that both tensile strain ε_{TC} and the critical strain ε_0 increase with the effective confining pressure increasing. The effect of the effective confining pressure on both tensile strain ε_{TC} and the critical strain ε_0 is not significant when it less than 10MPa, which agrees with observations reported by Fujii et al[3),9),10),11)] for 4 kinds of rocks under a confining pressure less than 20Mpa, and by Sakurai et al.[12)] for a porous tuff under that less than 0.6MPa.

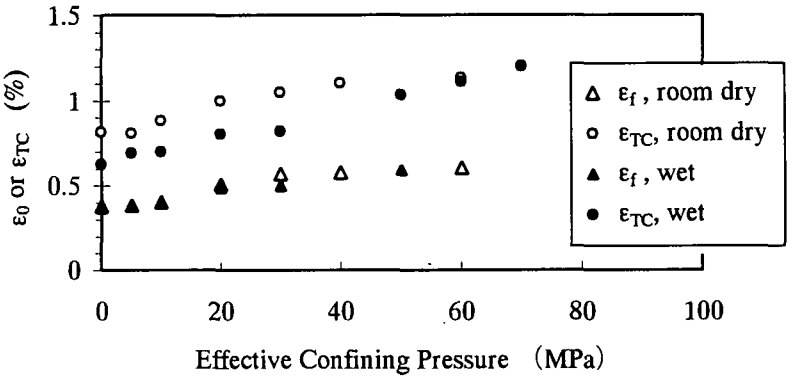

Fig.6 Effect of effective confining pressures (Shirahama sandstone I)

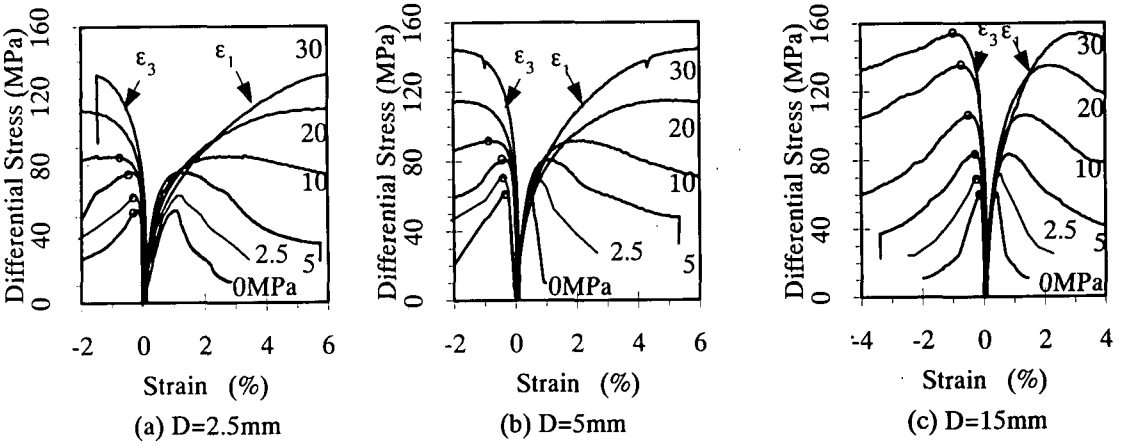

Fig.7 Stress-strain curves for concrete with different maximum sizes of aggregates(strain rate: 10με/s)

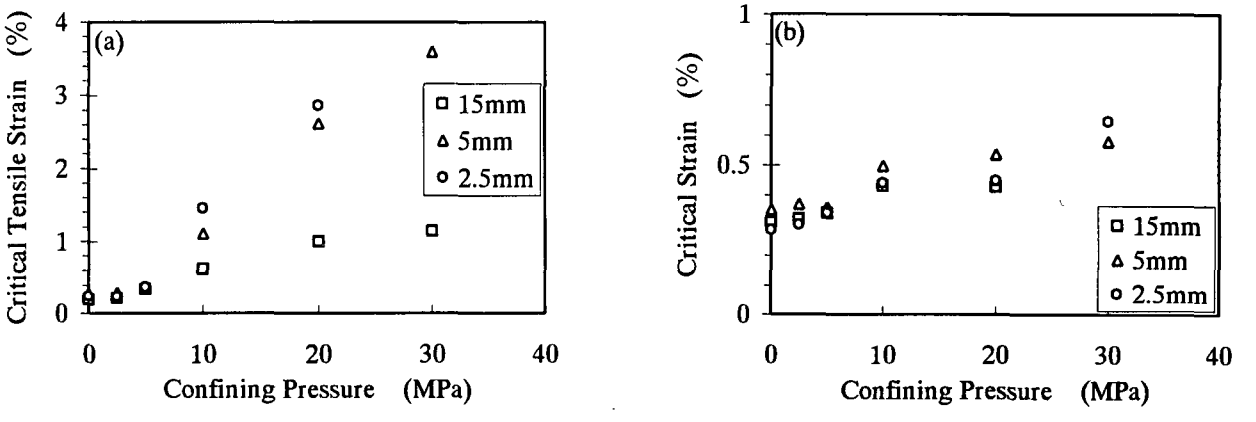

Fig.8 Effect of confining pressure on the critical tensile strain(a) and the critical strain(b) for the concrete with different max. aggregate size

As shown in Fig.6, the tensile strain ε_{TC} shows almost same value whether the pore pressure is present or not, however the critical strain ε_0 in room dry case shows a higher value than that with the pore pressure present.

3.2 Conventional Triaxial Tests for Concrete: Effects of Strain Rate, Confining pressure and Maximum Aggregate Size

gregate Size

The room dry concrete with maximum aggregate sizes of 2.5, 5, 15mm has been deformed under conventional triaxial compressions up to a maximum confining pressure of 30MPa. Fig.7 shows the stress-strain curves. A previous study has revealed that the brittle-ductile transition occurred at a confining pressure of 5-10MPa. According to the stress-strain curves measured, the

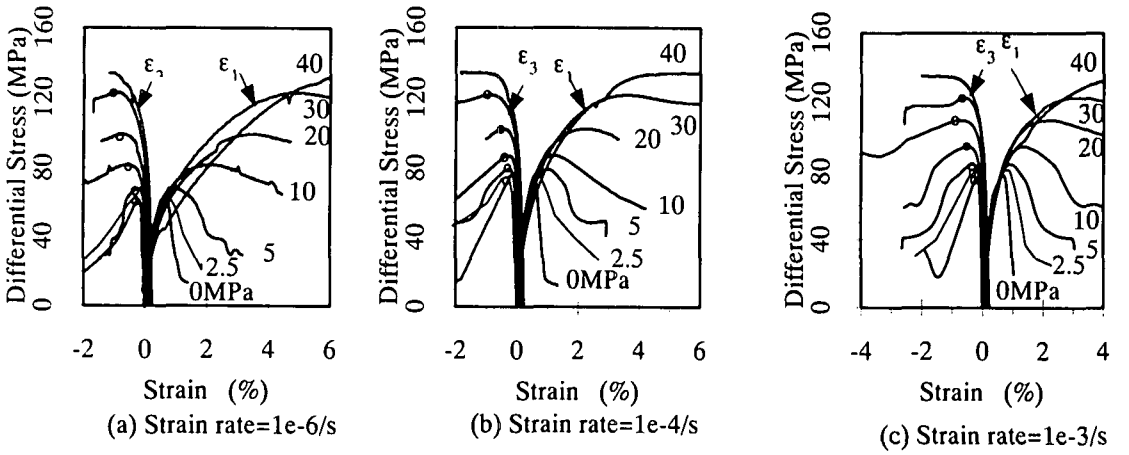

Fig.9 Stress-strain curves for concrete with a max. size of 1.2mm under different strain rates

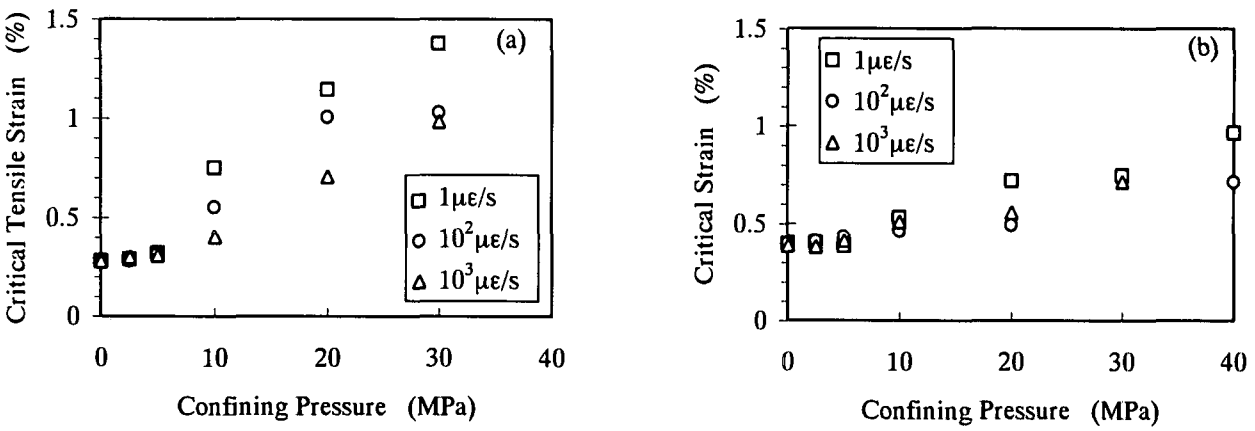

Fig.10 Effect of confining pressure on the critical tensile strain(a) and the critical strain(b) under differnet strain rates for the concrete with max. aggregate size of 1.2mm

tensile strain ε_{TC} and the critical strain ε_0 have been plotted as the functions of the confining pressure in terms of the maximum aggregate sizes(Fig.8). It can be seen that confining pressure affected ε_{TC} and ε_0 in a similar manner to that for Shiraham sandstone I (Fig.6). At a confining pressure less than 5MPa, in the range of brittle regime, the effects of both confining pressure and maximum aggregate size on ε_{TC} and ε_0 are not significant. At a higher confining pressure, the maximum aggregate size has a remarkable effect on ε_{TC}, but not remarkable on ε_0.

The effect of strain rate on the tensile strain ε_{TC} and the critical strain ε_0 for mortar with a maximum aggregate size of 1.2mm under triaxial compressions has been investigated. The strain rate ranges from 1-1000με/s, and confining pressure , from 0 to 40MPa. The differential stress has been plotted as a function of strains in Fig.9. Also, ε_{TC} and ε_0 have been plotted as the functions of confining pressure in terms of the strain rates(Fig.10). As shown in the figures, at a confining pressure less than 5MPa, in the range of brittle regime, the effects of both confining pressure and the strain rate on ε_{TC} and ε_0 are not significant. At a higher confining pressure, the strain rate has a remarkable effect on ε_{TC}, but not remarkable on ε_0. Furthermore, the smaller the strain rate, the higher values ε_{TC} ,and ε_0 show.

3.3 Shirahama Sandstone II : Effect of Intermediate Principal Stress

True triaxial tests have been performed for 5 Shirahama sandstone II specimens, where the minimum principal stress was 20MPa for all the specimen, and the intermediate principal stress was 20, 60, 100 140 and 192.7MPa respectively. The differential maximum principal stress-strain curves have been potted in Fig.11. Here, the differential maximum principal stress means the maximum principal stress minus minimum principal stress. Like Fig.4 and Fig.5, the minimum principal strain is total strain, the others are differential strain. The figures in the Fig.9 indicate the values of the intermediate principal stresses. Based on these curves, values of ε_{TC} and the maximum strain at failure ε_{1f} ,which are those of ε_3 and ε_1 corresponding to the peak points , can be determined directly. In our true triaxial tests, the

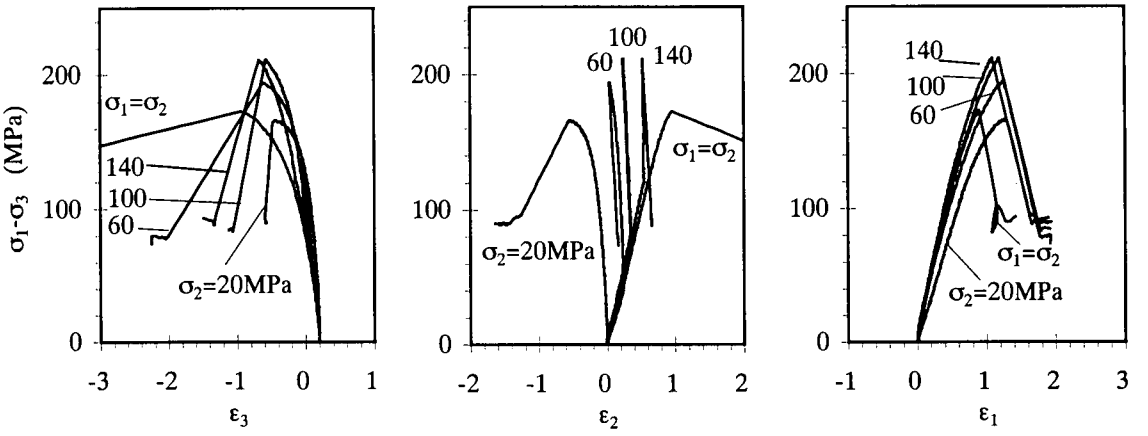

Fig.11 Differential maximun principal stress-strain curves under true triaxial stresses (Shirahama sandstone II, σ_3=20MPa)

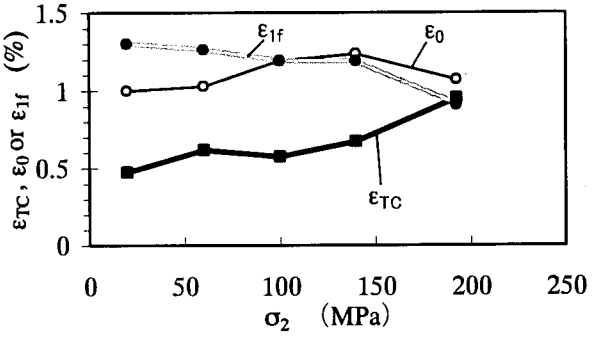

Fig.12 Effect of intermediate principal stresses for Shirahama sandstone II under true triaxial stresses (σ_3=20MPa)

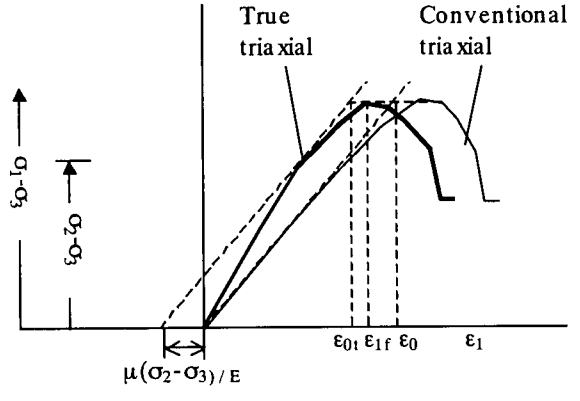

Fig.13 Definition of ε_{ot}

initial linear deformation was induced not only by σ_1 but also by σ_2. Thus, to evaluate ε_0, the modulus of deformation were calculated using Hook's law. ε_{TC}, ε_{1f} and ε_0 are plotted as the function of the intermediate principal stress in Fig.12.

It can be seen that the tensile critical strain of ε_{TC} increases with the intermediate principal stress σ_2 increasing, especially when σ_2 >100MPa .

The critical strain ε_0 , at first, increases, then, decreases with the intermediate principal stress increasing. Note that ε_0 become higher than the maximum strain at failure ε_{1f} when σ_2 >100MPa. Cautions should be given to this, because ε_0 is taken as a safety management index, should no less than ε_{1f} .

3.4 Definition of the critical strain under true triaxial stresses

As the above experimental results revealed, both the tensile strain ε_{TC} and the critical strain ε_0 are not sensitive to confining pressure, intermediate principal stress, strain rate and maximum aggregate size under low confining pressure and intermediate principal stress. However, the critical strain ε_0 become higher than the maximum strain at failure ε_{1f} when σ_2 >100MPa, which suggests that ε_0 defined as equation(4) may over-estimate the load-bearing capacity. Fig.13 shows the interpretation of the reason for this. Loading of σ_2 may reduce ε_1 by a quantity of

$\mu(\sigma_2 - \sigma_2)/E$, resulting from Poisson effect. Based on this analysis, we propose a new definition of the critical strain under true triaxial stresses ε_{0t} as the following equation.

$$\varepsilon_{0t} = \left[(\sigma_1 - \sigma_3)_f - \mu \cdot (\sigma_2 - \sigma_3)_f\right] / E \qquad (5)$$

where $(\sigma_1-\sigma_2)_f$ and $(\sigma_2-\sigma_3)_f$ are the differential maximum principal stress and the differential intermediate principal stress at failure respectively, E and μ are deformation modulus and Poisson's ratio respectively. Equation(5) means that failure occurs when the elastic portion of the maximum principal strain caused from the differential stresses reaches a critical value.

The critical strain ε_{0t} defined by equation(5), together with ε_0 defined by equation(4) and the maximum strain at failure ε_{1f} have been plotted as the functions of the intermediate principal stress σ_2 in Fig.14. It is apparent that ε_{0t} is affected by σ_2 to a less extent than ε_0, and furthermore always lower than ε_{1f}.

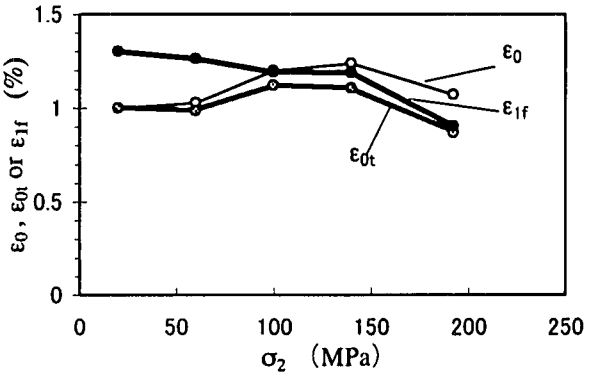

Fig.14 Effect of intermediate principal stresses for Shirahama sandstone II under true triaxial stresses (σ_3=20MPa)

4 Conclusions

In the present study, the effects of confining pressure, presence of pore pressure, intermediate principal stress, strain rate and maximum aggregate size on the tensile strain ε_{TC} and the critical strain ε_0 have been investigated by performing conventional and true triaxial tests for 2 kinds of Shirahama sandstone and 4 kinds of concrete.

The experimental results revealed that both the tensile strain ε_{TC} and the critical strain ε_0 are not affected significantly by confining pressure, intermediate principal stress, strain rate and maximum aggregate size under low confining pressure and intermediate principal stress.

However, the critical strain ε_0 become higher than the maximum strain at failure ε_{1f} when σ_2 >100MPa, which suggests that ε_0 defined as equation(3) may over-estimate the load-bearing capacity. In view of this analysis, a new definition for the critical strain has been proposed, which considers the effect of intermediate principal stress. The proposed definition has a clearer physical meaning and affected by the intermediate principal stress to a less extent than the original one.

REFERENCES

1) Hoek, E. and Brown, E. T. : Underground Excavations in Rocks, Inst. Min. Metall. , London, 1980.
2) Chen, W. F.: Concrete plasticity: past, present and future, in Strength Theory-Application, Development and Prospect for 21st century(Yu, M. eds), Science Press, Beijing, 1998.
3) Fujii, Y., Kiyama, T. and Ishijima, Y.: A study on tensile strain criterion, J. of The Mining and Materials Processing Institute of Japan, Vol.110, pp212-214,1994.
4) Sakurai, S.: An evaluation technique of displacement measurements in tunnels, J. of Geotechnical Engineering, No.317, pp.93-100, 1982.
5) Nadai, A.: Theory of flow and fracture of solids, Vol.1, 2nd Edition, McGrow Hill, New York, pp207-209, 1950.
6) Carino, N. J. and Slate, F. O.: J. Am. Concrete Inst.,Vol.73,pp160-165, 1976
7) Kotte, J. J., Berczes, Z. G., Gramberg, J. and Seldenrath, Th. R.: Int. j. Rock Mech. Min. Sci., Vol.6, pp581-595, 1969.
8) Stacey, T. R.: Int. j. Rock Mech. Min. Sci. &Geomech Abstr, Vol.18, pp469-474, 1981.
9) Kiyama, T. et al: Critical tensile strain and triaxial creep properties for Inada granite, Proc. of 94 Summer Symposium of Resources and Materials of Japan, pp101-102, 1994.
10) Fujii, Y., Kiyama, T. and Ishijima, Y.: New flailure criterion for rock, J. of The Mining and Materials Processing Institute of Japan, Vol. 109, pp549-550, 1993.
11) Fujii , Y . , Kiyama , T . and Ishijima , Y . : A new criterion for brittle failure of rock, Proc. MMIJ / AusIMM Joint Symp . ,Ube , Japan, 1994 .
12) Sakurai, S., Kawashima, I. And Otani, T.: Effects of environmental factors on critical strain of rocks, J. of Geotechnical Engineering, No.463/III-22, pp. 177-180, 1993.

(Received April 21, 2000)